Eur. Phys. J. E **14**, 127–135 (2004)
DOI 10.1140/epje/i2003-10141-4

THE EUROPEAN PHYSICAL JOURNAL E

Stationary shear flows of dense granular materials: A tentative continuum modelling

C. Josserand, P.-Y. Lagrée[a], and D. Lhuillier

Laboratoire de Modélisation en Mécanique, UMR 7607, Université P. et M. Curie (Paris 6) and CNRS, Boîte 162, 4 place Jussieu, 75252 Paris cedex 05, France

Received 17 December 2003 and Received in final form 24 March 2004 /
Published online: 29 June 2004 –

Abstract. We propose a simple continuum model to interpret the shearing motion of dense, dry and cohesion-less granular media. Compressibility, dilatancy and Coulomb-like friction are the three basic ingredients. The granular stress is split into a rate-dependent part representing the rebound-less impacts between grains and a rate-independent part associated with long-lived contacts. Because we consider stationary flows only, the grain compaction and the grain velocity are the two main variables. The predicted velocity and compaction profiles are in apparent qualitative agreement with most of the experimental or numerical results concerning free-surface shear flows as well as confined shear flows.

PACS. 45.70.Ht Avalanches – 45.70.-n Granular systems – 83.80.Fg Granular solids

1 Introduction

The mechanical behaviour of a flowing granular material depends strongly on the grain volume fraction. While dense granular media usually exhibit relatively slow motions with predominance of friction, less dense ones are usually found in vigorous motions with predominance of two-particles collisions. The collision-dominated regime is well described by kinetic theory, with the concepts of granular temperature and inelastic collisions. On the contrary, the current description of dense granular flows is not so fully satisfactory. It must be understood that we are not questioning the description by soil mechanics of quasi-static and highly stressed granular materials, but the description of flows with relatively low stress levels encountered, for example, in avalanches down an inclined plane. Several recent works (see, *e.g.* [1–3]) presented mitigated opinions about the possibility of describing dense granular flows within the realm of continuum mechanics. In fact, the experimental observation that many dense flows display a typical thickness of a few grain diameters must not be a factor of pessimism. We know from several examples in suspension mechanics that the continuum approach can cope with high-velocity gradients in one direction, provided one has some statistical homogeneity in the other two directions. This situation is exactly the one met in sheared granular media, provided we discard transient effects and focus on the final stationary state.

Once the principle of a continuum mechanical description is accepted, the number of relevant field variables must be decided. There is no doubt that the grain velocity is relevant but it is not less clear that *the grain volume fraction is also a pertinent variable*. In fact, the widely used assumption of an incompressible medium is not tenable. It contradicts the dilatancy concept and, as will be seen below, the transport coefficients of a dense granular medium display enormous variations with only tiny modifications of the compaction. Our aim is thus to propose a model for dense and stationary shear flows in which the grain compaction and the grain velocity are the two fundamental variables. One could also suggest the fluctuational kinetic energy of the grains (the granular "temperature") as a third variable. The main issue concerning the temperature of dense granular media is its dependence on the mean angular velocity of the grains, besides the more traditional fluctuations of their translational velocity. The description of non-stationary flows of dense media requires not only the resolution of the angular-momentum conservation equation but also the resolution of an equation for the fluctuations of angular velocity. To bypass these complex issues, we focus henceforth on stationary flows and assume the equality between the mean angular velocity of the grains and the angular velocity of the granular medium as a whole. As a consequence, the generalized granular temperature is no longer an independent state variable, but a function of the solid fraction and of the symmetric velocity gradient only.

[a] e-mail: pyl@ccr.jussieu.fr

The role of the embedding fluid will be neglected everywhere, and for these "dry" granular media, the main issue is to propose a constitutive relation for the granular stress. To compare with previous works on dense flows, we can say we adopt a phenomenological description somewhat similar to that proposed two decades ago by Savage [4] and by Johnson and Jackson [5]. Like these authors, we introduce a stress tensor split into a frictional and a collisional contribution. However, the collisional contribution is concerned with rebound-less impacts typical of high grain concentration, and is free of any restitution coefficient [2]. Our constitutive relation for the particulate stress has a form somewhat similar to that proposed by Ancey and Evesque [6], the main differences concerning the explicit role of the grain compaction and a more detailed expression of the granular pressure. Our model also shares some common features with the model proposed by Bocquet *et al.* [7], but instead of extending the kinetic theory approach to large compaction, we prefer here to develop a model specifically devoted to dense media. In other words, we share with Bocquet *et al.* the opinion that high-density granular materials need a special expression for the viscosity coefficient. But, we claim with Savage and Johnson and Jackson that dense granular materials also need a special expression for the grain pressure in order to mimic the role of contact forces between grains. Moreover, the model we propose is quite simple insofar as it denies any special role to the compaction gradient [8] and avoids the non-locality concept [9].

Discarding two-particles collisions and any restitution coefficient means that our model is restricted to volume fractions in the range between $\phi_{\rm m}$ and $\phi_{\rm M}$. The maximum grain compaction $\phi_{\rm M}$ corresponds to the highest possible random packing (with $\phi_{\rm M} \simeq 0.80$ for two-dimensional flows and $\phi_{\rm M} \simeq 0.65$ for three-dimensional ones) while $\phi_{\rm m}$ is the smallest compaction compatible with the existence of a continuous network of contacts between grains. As suggested by Azanza [1], one can define $\phi_{\rm m}$ as the minimum compaction for which the two-particle distribution function exhibits some swelling at a distance of *two* diameters. With this definition, $\phi_{\rm m} \simeq 0.70$ for two-dimensional flows, while $\phi_{\rm m} \simeq 0.50$ for three-dimensional ones.

A phenomenological order parameter description of granular media was recently proposed [10]. We acknowledge this approach looks efficient and we agree with Volfson *et al.* that the fraction of solid contacts is a possible order parameter, but we also claim that a much simpler order parameter exists which is the reduced compaction $(\phi-\phi_{\rm m})/(\phi_{\rm M}-\phi_{\rm m})$. And since the solid fraction ϕ obeys a conservation equation, we do not have to worry about the Ginzburg-Landau equation. Stated differently, we consider the solid fraction as a pertinent variable (or the reduced compaction as a pertinent order parameter) and we want to present the potentialities of such an assumption.

The description of stationary free-surface shear flows is given in Section 2 while that of confined shear flows is presented in Section 3. Section 4 compares the model predictions with experimental and (or) numerical data. The final section insists on the limitations and necessary improvements of the proposed model, which must be considered as a minimal one.

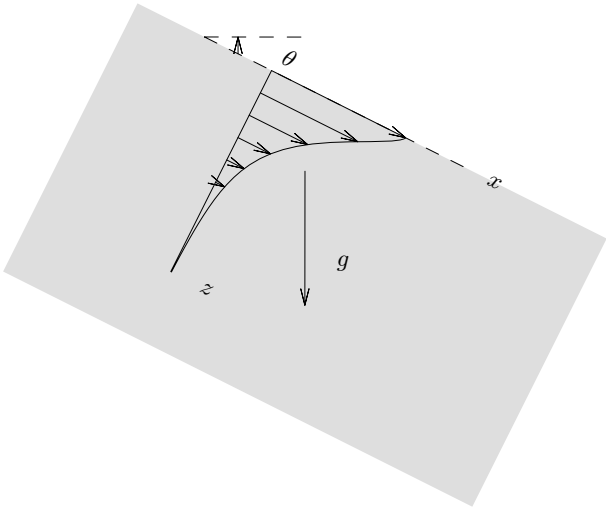

Fig. 1. Gravity-induced shear flow with free surface (over a heap or an inclined plate with an angle θ relative to the horizontal plane).

2 Free-surface shear flows

As a prototype of shear flow with free surface, we consider the gravity-induced chute (over a heap or an inclined plate, see Fig. 1) with an angle θ relative to the horizontal plane. The mean grain velocity is parallel to the x-axis, $\mathbf{V} = V\mathbf{e}_x$, while V and the solid fraction ϕ depend only on z, the *distance to the free surface*. The granular stress tensor is noted τ and the equations of motion are:

$$0 = -\frac{\partial \tau_{xz}}{\partial z} + \phi\rho g \sin(\theta) \ , \quad 0 = -\frac{\partial \tau_{zz}}{\partial z} + \phi\rho g \cos(\theta) \ , \quad (1)$$

where ρ is the constant mass per unit volume of the grain material and g is the acceleration of gravity.

For dense granular media, the granular stress is a consequence of long-lived contacts and bounce-less impacts between grains. Long-lived contacts result from compressive forces acting towards the boundaries of the granular medium. In the geometry considered, they take part in τ_{zz} since z is the direction of main compression. Whether gravity is responsible for compressive forces or not, we choose to scale the compressive stress with $\rho g D$, where D is the grain size. The compressive stresses are related to the grain volume fraction as $\rho g D F(\phi)$, where $\mathrm{d}F/\mathrm{d}\phi$ is the non-dimensional rigidity of the granular medium. In free-surface shear flows, gravity is the only source of compaction and the magnitude of the compressive stress will also depend on θ. It is clear that the compressive role of gravity is maximum when the compression axis z is vertical, while this role vanishes when gravity is orthogonal to it. Consequently, the general form of the gravity-induced compressive stress is $\rho g D F(\phi) f(\theta)$ with $f(0) = 1$

and $f(\pi/2)= 0$. The exact expression of $f(\theta)$ is not important because, as will soon be seen, the stationary flows exist in a very limited range of θ only. One of the simplest function of θ which meets the above requirement is $\cos(\theta)$, and we assume henceforth that the contribution of long-lived contacts to τ_{zz} can be written in the form $\rho g D F(\phi)\cos(\theta)$. To this gravity-induced contact stress a rate-dependent impact stress must be added. On purely dimensional grounds, this second contribution cannot be but Bagnold-like and the full normal stress finally appears in the form

$$\tau_{zz} = \rho D^2 \mu_{\rm N}(\phi) \left(\frac{{\rm d}V}{{\rm d}z}\right)^2 + \rho g D F(\phi)\cos(\theta), \qquad (2)$$

where $\mu_{\rm N}(\phi)$ represents the compaction-dependent intensity of the normal stress induced by the shear rate. Concerning the shear stress of the flowing granular medium, we assume it is made of a Coulomb-like contribution with a friction coefficient $\mu(\phi)$ completed by a Bagnold-like contribution involving a coefficient $\mu_{\rm T}(\phi)$ representing the compaction-dependent intensity of the shear stress induced by the shear rate

$$\tau_{xz} = \rho D^2 \mu_{\rm T}(\phi) \left(\frac{{\rm d}V}{{\rm d}z}\right)^2 + \mu(\phi)\tau_{zz}. \qquad (3)$$

The model expressions (2) and (3) contain four functions of the grain compaction. Before giving them some explicit (and tentative) expressions, let us comment on their expected general behaviour. These four functions describe the dense regime and have a meaning in the range $\phi_{\rm m} \le \phi \le \phi_{\rm M}$ only. We expect F, $\mu_{\rm T}$ and $\mu_{\rm N}$ to become infinite when $\phi = \phi_{\rm M}$, because no motion nor extra compaction is expected above the maximum random packing. We also expect F and $\mu_{\rm N}$ to vanish for $\phi = \phi_{\rm m}$, because the normal stresses must vanish for the most tenuous contact network. Concerning the friction coefficient μ, it is the only coefficient which remains finite when $\phi = \phi_{\rm M}$ and it presumably increases [11] for smaller compactions. In short, the three scalars F, $\mu_{\rm N}$ and $\mu_{\rm T}$ are strongly increasing functions of the compaction, while μ has a much smoother behaviour.

Since we neglect the role of the embedding fluid, the granular stress must vanish at the free surface and consequently $\tau_{xz} = \tan(\theta)\tau_{zz}$ everywhere. In this case, when solving the equations of motion (1) with the model expressions (2) and (3), one arrives at a compaction profile and a velocity profile which are solution of

$$D\frac{{\rm d}\phi}{{\rm d}z} = \frac{\phi}{\dfrac{\partial}{\partial\phi}\left[\dfrac{F}{1-(\mu_{\rm N}/\mu_{\rm T})(\tan(\theta)-\mu)}\right]} \qquad (4)$$

and

$$\left(\frac{D}{g}\right)^{1/2}\frac{{\rm d}V}{{\rm d}z} = -\left(\frac{F(\sin(\theta)-\mu\cos(\theta))}{\mu_{\rm T}(1-(\mu_{\rm N}/\mu_{\rm T})(\tan(\theta)-\mu))}\right)^{1/2}. \qquad (5)$$

At the free surface the solid fraction is $\phi_{\rm m}$ (remember we limit the description to the dense regime and discard all phenomena acting for solid fractions less than $\phi_{\rm m}$). According to (4) the solid fraction increases towards its maximum value $\phi_{\rm M}$ over a depth which scales with the grain diameter but depends on θ if $\mu_{\rm N}/\mu_{\rm T}$ is different from zero. Hence, $\mu_{\rm N}/\mu_{\rm T}$ represents the relative magnitude of Reynold's dilatancy. Concerning the velocity profile, its characteristic value scales like $(gD)^{1/2}$ and according to (5) its solution exists for any angle θ verifying the inequality $\mu(\phi) \le \tan(\theta) \le \mu(\phi) + \mu_{\rm T}(\phi)/\mu_{\rm N}(\phi)$. For certain values of θ this inequality is possibly satisfied in a part only of the full range $\phi_{\rm m} \le \phi \le \phi_{\rm M}$.

It is obviously not evident to deduce four functions of the compaction from the rather scarce experimental or numerical results on stationary shear flows. *We assume henceforth that* μ and $\mu_{\rm T}/\mu_{\rm N}$ *are independent of the grain compaction.* Then, a stationary solution is possible in a well-defined angle range $\theta_{\rm min} \le \theta \le \theta_{\rm max}$, with $\tan(\theta_{\rm min}) = \mu$ and $\tan(\theta_{\rm max}) = \mu + \mu_{\rm T}/\mu_{\rm N}$. To obtain more quantitative results, we consider separately the chute over a heap from that over an inclined plane.

2.1 Heap flows

In the heap case, provided μ and $\mu_{\rm N}/\mu_{\rm T}$ are independent of the solid fraction, one can deduce from (4) and (5) the total granular flux flowing down the heap $Q_{\rm heap}$:

$$\frac{Q_{\rm heap}}{D\sqrt{gD}} = \frac{(\sin(\theta)-\mu\cos(\theta))^{1/2}}{\left(1-\frac{\mu_{\rm N}}{\mu_{\rm T}}(\tan(\theta)-\mu)\right)^{5/2}} \int_{\phi_{\rm m}}^{\phi_{\rm M}} \left(\frac{F^3}{\mu_{\rm T}}\right)^{1/2} \frac{\partial F}{\partial\phi}\frac{{\rm d}\phi}{\phi}, \qquad (6)$$

the grain velocity $V_{\rm heap}(0)$ at the free surface,

$$\frac{V_{\rm heap}(0)}{\sqrt{gD}} = \frac{(\sin(\theta)-\mu\cos(\theta))^{1/2}}{\left(1-\frac{\mu_{\rm N}}{\mu_{\rm T}}(\tan(\theta)-\mu)\right)^{3/2}} \int_{\phi_{\rm m}}^{\phi_{\rm M}} \left(\frac{F}{\mu_{\rm T}}\right)^{1/2} \frac{\partial F}{\partial\phi}\frac{{\rm d}\phi}{\phi} \qquad (7)$$

and the relative velocity profile

$$\frac{V_{\rm heap}(z)}{V_{\rm heap}(0)} = \frac{\int_{\phi_{\rm heap}(z)}^{\phi_{\rm M}} \left(\frac{F}{\mu_{\rm T}}\right)^{1/2} \frac{\partial F}{\partial\phi}\frac{{\rm d}\phi}{\phi}}{\int_{\phi_{\rm m}}^{\phi_{\rm M}} \left(\frac{F}{\mu_{\rm T}}\right)^{1/2} \frac{\partial F}{\partial\phi}\frac{{\rm d}\phi}{\phi}}. \qquad (8)$$

Since the free-surface velocity and the flux are expected to have finite values for $\theta_{\rm min} < \theta < \theta_{\rm max}$, the two functions $F(\phi)$ and $\mu_{\rm T}(\phi)$ must be such as to guarantee the convergence of the above integrals. In this case $V_{\rm heap}(0)$ and $Q_{\rm heap}$ are functions of θ with numerical prefactors depending on one's peculiar choice for F and $\mu_{\rm T}$. In what follows, we adopt the simple expressions

$$F = F_0 {\rm Log}\left(\frac{\phi_{\rm M}-\phi_{\rm m}}{\phi_{\rm M}-\phi}\right) \text{ and } \mu_{\rm T} = \mu_{\rm T0}\left(\frac{\phi_{\rm M}-\phi_{\rm m}}{\phi_{\rm M}-\phi}\right)^2. \qquad (9)$$

The same expression for F was already proposed by Savage [4,12] and we comment on it in Appendix A. A more general expression for $\mu_{\rm T}$ and its consequences are described in Appendix B. The above expression for F leads

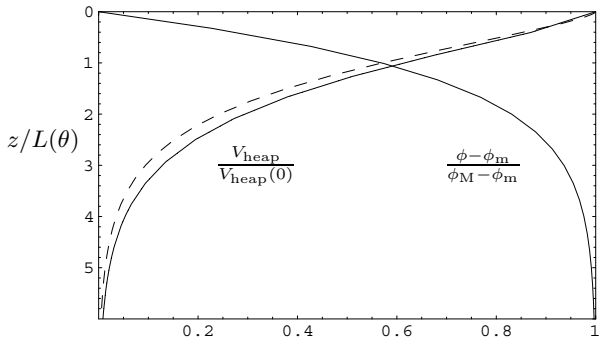

Fig. 2. Reduced velocity profile $V_{\rm heap}/V_{\rm heap}(0)$ *versus* the adimensional distance $z/L(\theta)$ to the free surface. The dashed curve represents the approximate expression (12). The reduced compaction profile $(\phi-\phi_{\rm m})/(\phi_{\rm M}-\phi_{\rm m})$ is plotted as well.

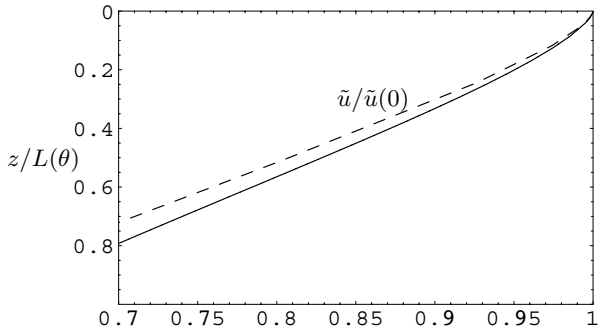

Fig. 3. Zoom of Figure 2 showing the Bagnold-like region for $z/L(\theta) < 0.2$. The dashed curve represents approximation (12).

to a solid fraction profile which increases exponentially with depth:

$$\phi_{\rm heap}(z,\theta) = \frac{\phi_{\rm M}}{1+(\frac{\phi_{\rm M}}{\phi_{\rm m}}-1)e^{-z/L(\theta)}}\,, \qquad (10)$$

where

$$L(\theta) = \frac{F_0 D}{\phi_{\rm M}(1-\frac{\mu_{\rm N}}{\mu_{\rm T}}(\tan(\theta)-\mu))} \qquad (11)$$

represents the typical thickness of the layer flowing down the heap. The relative velocity profile deduced from the above expressions for F and $\mu_{\rm T}$ is exponential-like for $\frac{z}{L(\theta)} \gtrsim 2$ (see Fig. 2) but displays a Bagnold-like region of inverse concavity for $\frac{z}{L(\theta)} \lesssim 0.2$ (see Fig. 3). In fact, our numerical solution for the relative velocity profile is quite well fitted by the analytical expression

$$1-\frac{V_{\rm heap}(z)}{V_{\rm heap}(0)} = \left(\frac{\phi_{\rm heap}(z)-\phi_{\rm m}}{\phi_{\rm M}-\phi_{\rm m}}\right)^{\frac{3}{2}} = \left(\frac{1-e^{-z/L(\theta)}}{1+(\frac{\phi_{\rm M}}{\phi_{\rm m}}-1)e^{-z/L(\theta)}}\right)^{\frac{3}{2}}. \qquad (12)$$

With $\phi_{\rm m}=0.5$ and $\phi_{\rm M}=0.65$ the total flux flowing down the heap is

$$\frac{Q_{\rm heap}}{D\sqrt{gD}} = 1.4\frac{F_0^{5/2}}{\mu_{\rm T0}^{1/2}}\frac{(\sin(\theta)-\mu\cos(\theta))^{1/2}}{\left(1-\frac{\mu_{\rm N}}{\mu_{\rm T}}(\tan(\theta)-\mu)\right)^{5/2}}.$$

The dependence on θ of L and $Q_{\rm heap}$ are represented in Figure 4, with $\mu=0.36$ and $\mu_{\rm N}/\mu_{\rm T}=4.7$.

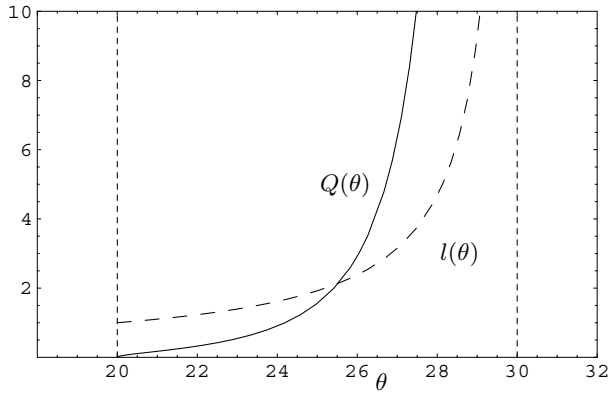

Fig. 4. θ-dependence of flux $Q_{\rm heap}$ and adimensional thickness $l(\theta)=\phi_{\rm M}L(\theta)/D$.

2.2 Chute on rough plates

The flows over inclined rough plates are more difficult to handle because the constitutive equations (2) and (3) hold in the bulk only of the dense granular medium and are likely to be modified close to the rough plate. Since the role of the plate rugosity is difficult to assess quantitatively, we discard the description of the "basal layer" close to the plate [6,13] and assume a slip velocity $V_{\rm s}$ at some distance δ above the rough plate. Then, we apply (2) and (3) to a layer of thickness h, so that the free surface is located at a distance $h+\delta$ above the rough incline. In the layer of thickness h, the solid fraction increases from $\phi_{\rm m}$ at the free surface to the value $\phi_{\rm heap}(h)$ at a distance δ from the rough plate, where the velocity is $V_{\rm s}$. The total flux through the core region is now given by:

$$\frac{Q_{\rm plate}}{D\sqrt{gD}} = \frac{F(\phi_{\rm heap}(h))}{1-\frac{\mu_{\rm N}}{\mu_{\rm T}}(\tan(\theta)-\mu)}\frac{V_{\rm s}}{\sqrt{gD}} + \frac{(\sin(\theta)-\mu\cos(\theta))^{1/2}}{\left(1-\frac{\mu_{\rm N}}{\mu_{\rm T}}(\tan(\theta)-\mu)\right)^{5/2}} \times \int_{\phi_{\rm m}}^{\phi_{\rm heap}(h)}\left(\frac{F^3}{\mu_{\rm T}}\right)^{1/2}\frac{\partial F}{\partial\phi}\frac{{\rm d}\phi}{\phi}. \qquad (13)$$

A rough plate is likely to slow down the core region more efficiently than a heap would do and we expect $V_{\rm s} \le V_{\rm heap}(h)$. As a consequence, $Q_{\rm plate}(h,\theta)$ as given in (13) is not expected to exceed $Q_{\rm heap}(\theta)$ given in (6). When *forcing* a flux $Q_{\rm plate}$ to flow down a rough plane inclined at angle θ, two different situations are encountered: when $Q_{\rm plate}$ is larger than $Q_{\rm heap}(\theta)$, the granular medium

will re-arrange so as to flow down over a heap of angle $\theta + \alpha$ with $Q_{\rm plate} = Q_{\rm heap}(\theta + \alpha)$. This gives a possible explanation for the "immature sliding flows" that were observed in some experiments [3,4]. Due to the very large increase of $Q_{\rm heap}$ with θ (see Fig. 4) and because the experimental flux is limited to some maximal value, immature sliding flows were observed for small angles close to $\theta_{\rm min}$ only. Conversely, when $Q_{\rm plate}$ is smaller than $Q_{\rm heap}(\theta)$, the whole layer of thickness h is in motion with a velocity everywhere larger than $V_{\rm s}$. Moreover, when $h/L(\theta) \lesssim 0.2$, the Bagnold-like velocity profile (which could hardly be observed in heap flows, see Fig. 3) is now invading the whole core region. In fact, when expressions (9) are taken for granted and $h/L(\theta) \lesssim 0.2$, the total flux (13) has the special form

$$\frac{Q_{\rm plate}}{D\sqrt{gD}} = \frac{\phi_{\rm m} V_{\rm s} h}{D\sqrt{gD}} + \frac{2}{5}\phi_{\rm m}^{3/2}\left(\frac{(\sin(\theta) - \mu\cos(\theta))}{\mu_{\rm T0}}\right)^{1/2}\left(\frac{h}{D}\right)^{5/2}. \tag{14}$$

When the role of the velocity slip can be neglected, the second contribution gives a $h^{5/2}$ scaling law for the grain flux down a rough incline. Note that this scaling stems from our particular choice (9). The consequences of a different choice for $\mu_{\rm T}$ are analyzed in Appendix B.

3 Confined shear flow

In the two-dimensional shear flows we will consider, the pressure load exerted on the boundaries of the granular medium is supposed to be applied along direction z, which is thus the direction of main compression. Because gravity plays a minor role concerning the compressive forces, the constitutive relation for τ_{zz} is simply (compare with (2))

$$\tau_{zz} = \rho D^2 \mu_{\rm N}(\phi)\left(\frac{{\rm d}V}{{\rm d}z}\right)^2 + \rho g D F(\phi), \tag{15}$$

whatever the angle θ between the z-axis and gravity. The flow is along the x-axis and the constitutive relation for the shear stress τ_{xz} is still given by (3), without any change as compared to the free-surface case.

3.1 Plane shear flow

As a first type of confined shear flow, we consider the planar shear of an infinite horizontal granular layer bounded by two plates separated by a *fixed distance* h. The pressure load and the gravity are both oriented along the direction z and the flow is along direction x (see Fig. 5). The equations of motion result in a constant shear stress S and a variable normal stress

$$\tau_{xz} = S \;\text{ and }\; \tau_{zz}(z) = P(0) + \rho g \int_0^z \phi(\xi){\rm d}\xi\,,$$

where $P(0)$ is the pressure load exerted on the upper plate $z = 0$ ($z = h$ stands for the lower plate). We will distinguish the situation without and with gravity, the first case corresponding to numerical simulations and the second one to experiments.

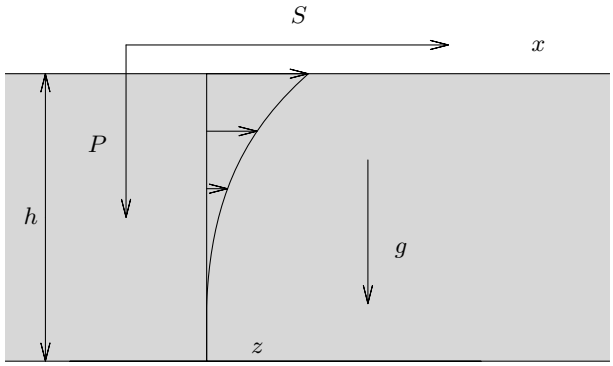

Fig. 5. Planar confined shear flow of an infinite horizontal granular layer bounded by two plates separated by a fixed distance h. The pressure load P and the gravity are both oriented along the direction z, the shear stress S and the flow are along direction x.

3.1.1 Without gravity

In this case the normal stress is also a constant P all over the granular layer and the constitutive equations (15) and (3) give

$$\rho D^2 \mu_{\rm T}(\phi)\left(\frac{\partial V}{\partial z}\right)^2 = S - \mu(\phi)P\,,$$
$$\rho D^2 \mu_{\rm N}(\phi)\left(\frac{\partial V}{\partial z}\right)^2 = P - \rho g D F(\phi)\,. \tag{16}$$

Depending on the sign of $S - \mu(\phi)P$, we will have a static or a moving medium. In the static case the pressure load is noted P_0 and the shear is such that $S \le \mu(\phi_0)P_0$, where ϕ_0 is the constant compaction of the medium related to the pressure load through $P_0 = \rho g D F(\phi_0)$. In the dynamic case the compaction is still a constant and because of mass conservation this constant is nothing but the static value ϕ_0. The shear S is now larger than $\mu(\phi_0)P_0$. The velocity gradient is constant:

$$\rho D^2\left(\frac{\partial V}{\partial z}\right)^2 = \frac{S - \mu(\phi_0)P_0}{\mu_{\rm T}(\phi_0) + \mu(\phi_0)\mu_{\rm N}(\phi_0)}\,.$$

Due to dilatancy effects the pressure load exerted on the plates is necessarily larger than in the static case, following:

$$P(S) = P_0 + \frac{S - \mu(\phi_0)P_0}{\mu(\phi_0) + \mu_{\rm T}(\phi_0)/\mu_{\rm N}(\phi_0)}.$$

As a consequence, the effective friction coefficient is a function of ϕ_0 and P:

$$\frac{S}{P} = \mu(\phi_0) + \frac{\mu_{\rm T}(\phi_0)}{\mu_{\rm N}(\phi_0)}\left(1 - \frac{\rho g D}{P}F(\phi_0)\right).$$

3.1.2 With gravity

In this case the normal stress increases in the downward direction so that the constitutive equation (3) results in

$$\rho D^2 \mu_{\rm T}(\phi) \left(\frac{\partial V}{\partial z}\right)^2 = S - \mu(\phi) P(0) - \mu(\phi)\rho g \int_0^z \phi(\xi) \mathrm{d}\xi \,.$$

It is then clear that the gravity-induced extra compaction possibly induces shear localization because *the right-hand side can have a different sign in different parts of the flow.* To simplify this issue, we will now introduce the same assumptions we have previously used in the free-surface shear flows, namely that μ and $\mu_{\rm T}/\mu_{\rm N}$ do not depend on ϕ, while $F(\phi)$ and $\mu_{\rm T}(\phi)$ are given by (9). We will first describe the static case before considering grain motions. Because the compaction on the upper plate is necessarily different in the static and the dynamic cases, we define $P_0(0)$ as the pressure load exerted on the upper plate when the granular medium is motionless and $\phi_0(z)$ as the static compaction profile. As long as $S \leq \mu P_0(0)$, the granular slab is motionless, the compaction $\phi_0(0)$ at the upper plate satisfies $P_0(0) = \rho g D F(\phi_0(0))$ and the compaction profile is

$$\phi_0(z) = \frac{\phi_{\rm M}}{1 + \left(\frac{\phi_{\rm M}}{\phi_0(0)} - 1\right) e^{-z/L_0}} \quad \text{with} \quad L_0 = \frac{F_0}{\phi_{\rm M}} D.$$

When the granular medium is flowing, the compaction profile $\phi(z)$ displays larger gradients and becomes

$$\phi(z) = \frac{\phi_{\rm M}}{1 + \left(\frac{\phi_{\rm M}}{\phi(0)} - 1\right) e^{-z/L}} \quad \text{with} \quad L = \frac{L_0}{1 + \mu \frac{\mu_{\rm N}}{\mu_{\rm T}}},$$

where $\phi(0)$ is the new compaction at the upper plate. Since mass conservation requires

$$\int_0^h [\phi(z) - \phi_0(z)] \mathrm{d}z = 0,$$

it is clear that the inequality $L < L_0$ implies $\phi(0) < \phi_0(0)$ and $\phi(h) > \phi_0(h)$. The compaction of the moving medium is thus reduced at the upper plate as compared to its static value while it is enhanced at the lower plate.

The velocity profile is then deduced from the compaction profile

$$\left(1 + \mu \frac{\mu_{\rm N}}{\mu_{\rm T}}\right) \frac{D}{g} \left(\frac{\partial V}{\partial z}\right)^2 = \frac{S^* - \mu F(\phi)}{\mu_{\rm T}(\phi)} \,,$$

where S^* is the dimensionless shear $\frac{S}{\rho g D}$. Let us define the volume fraction ϕ^* such that $S^* = \mu F(\phi^*)$. It is clear that $\phi^* > \phi_0(0)$, because $S > \mu P_0(0)$. The above equation implies that motion exists for compactions less than ϕ^* only. This condition leads to check the self-consistency relation $\phi(z) < \phi^*$ for $0 < z < h$. This condition is automatically satisfied in the upper part of the flow since $\phi(0) < \phi_0(0) < \phi^*$. But it may be not in the lower part, thus leading to a shear localization. This *bulk* localization is here depending on S^* and h/L. Figure 6 shows the compaction and velocity profiles for two different values of $\phi^*(S^*)$ representing the two different situations: shear localization or flow over the whole layer.

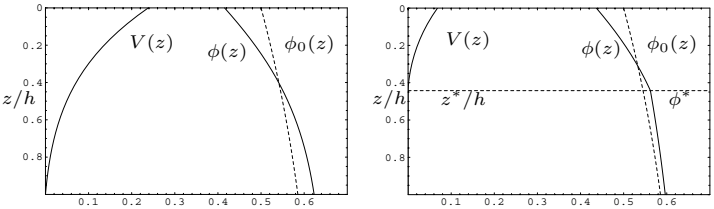

Fig. 6. Velocity profile $V(z)$ and compaction profile $\phi(z)$; left: large S; right: small S.

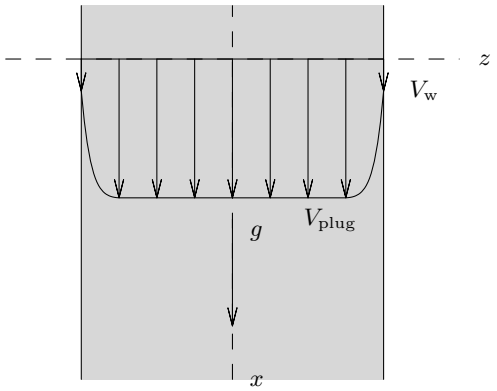

Fig. 7. Vertical chute flow between two rough plates.

3.2 Vertical chute flows

A second type of confined shear flow is the chute between two vertical plates (see Fig. 7). The compaction is due to a pressure load P exerted on the two plates along direction z. The flow and the gravity are oriented along direction x. The equations of motion result in a constant normal stress and a variable shear stress, by contrast to the preceding case:

$$\tau_{zz} = P \qquad \text{and} \qquad \tau_{xz} = \rho g \int_0^z \phi(\xi) \mathrm{d}\xi,$$

where $z = 0$ corresponds to the symmetry plane located between the two plates at which the shear stress vanishes. The constitutive relation (3) implies

$$\rho D^2 \mu_{\rm T}(\phi) \left(\frac{\partial V}{\partial z}\right)^2 = \rho g \int_0^z \phi(\xi) \mathrm{d}\xi - \mu(\phi) P.$$

Either the right-hand side is everywhere negative (due to a very high pressure load) and the medium is motionless or there is a central region of the flow in which the shear stress does not exceed μP and consequently where the strain rate vanishes. In this plug flow regime the solid fraction is a constant ϕ^* related to the pressure load as $P = \rho g D F(\phi^*)$. The thickness z^* of the plug flow depends on ϕ^* (hence on the pressure load):

$$\frac{z^*}{D} = \frac{\mu(\phi^*)}{\phi^*} F(\phi^*).$$

Close to the vertical plates, there is a shear layer where the velocity decrease to $V_{\rm w}$ dependent on the plate roughness.

In this parietal shear layer, the constitutive equations (15) and (3) imply

$$\left(\frac{D}{g}\right)^{1/2}\frac{\partial V}{\partial z} = -\left(\frac{F(\phi^*)-F(\phi)}{\mu_{\rm N}(\phi)}\right)^{1/2} \qquad (17)$$

and

$$D\frac{\partial \phi}{\partial z} = \frac{\phi}{\frac{\partial}{\partial \phi}\left[(\mu+\frac{\mu_{\rm T}}{\mu_{\rm N}})F(\phi^*)-\frac{\mu_{\rm T}}{\mu_{\rm N}}F(\phi)\right]}. \qquad (18)$$

To obtain more definite results, we again consider the assumptions already made for gravity-driven and plane shear flows, namely that μ and $\mu_{\rm N}/\mu_{\rm T}$ are independent of the solid fraction, while $F(\phi)$ and $\mu_{\rm T}(\phi)$ are given by (9). Then, the compaction profile in the shear layer $z^* < z < z_{\rm w}$ is

$$\phi(z) = \frac{\phi_{\rm M}}{1+\left(\frac{\phi_{\rm M}}{\phi^*}-1\right)e^{\frac{z-z^*}{L^*}}}, \qquad (19)$$

where L^* is the typical shear layer thickness:

$$\frac{L^*}{D} = \frac{\mu_{\rm T}F_0}{\mu_{\rm N}\phi_{\rm M}}.$$

For the flow to be dense up to the vertical plates, the wall compaction $\phi_{\rm w}$ must be larger than $\phi_{\rm m}$ and the shear layer thickness is

$$\frac{z_{\rm w}-z^*}{L^*} = Log\left(\frac{\frac{\phi_{\rm M}}{\phi_{\rm w}}-1}{\frac{\phi_{\rm M}}{\phi^*}-1}\right).$$

As a consequence, the distance $2z_{\rm w}$ between the two plates is a function of ϕ^* (hence of P) and of $\phi_{\rm w}$ (hence of the plate roughness). Concerning the velocity, it increases from a value $V_{\rm w}$ at the wall to a value $V_{\rm plug}$ in the central part. The computed relative velocity field is represented in Figure 8 together with the fit

$$\frac{V(z)-V_{\rm w}}{V_{\rm plug}-V_{\rm w}} = 1-\left(\frac{\phi^*-\phi(z)}{\phi^*-\phi_{\rm w}}\right)^{3/2}. \qquad (20)$$

4 Qualitative comparison with experimental and (or) numerical data

Since many experimental and numerical data were reviewed in [14], we will often use this reference where the original works are quoted therein. Moreover the comparison between the model predictions and the experimental or numerical data will be qualitative only, our aim being to test the potentialities of the model rather than to give definite values to parameters such as F_0 or $\mu_{\rm T0}$.

4.1 Plane shear flow

Neglecting the influence of gravity (as was done in most numerical simulations) our model leads to a uniform solid fraction and to a uniform velocity gradient, in conformity with results presented in Figures 5b and c of [14] for the dense-flow regime. When gravity is taken into account, a shear localization is possible, depending on the magnitude of the pressure load as well as on the thickness of the granular layer. Unfortunately, we are unaware of experimental or numerical data with which the predictions of Figure 6 could be tested.

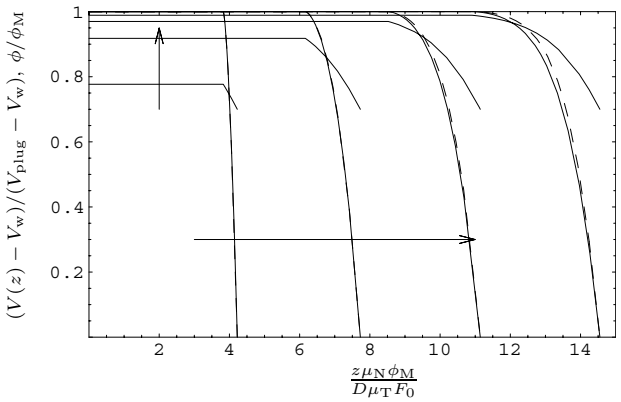

Fig. 8. Reduced velocity profiles $(V(z)-V_{\rm w})/(V_{\rm plug}-V_{\rm w})$ *versus* the adimensional distance $\frac{z\mu_{\rm N}\phi_{\rm M}}{D\mu_{\rm T}F_0}$ to the center. The arrows are in the increasing values of $\frac{P}{\rho g D F_0}$. The dashed curves represent the approximate expression (20). The reduced compaction profiles $\phi/\phi_{\rm M}$ with $\phi_{\rm w}/\phi_{\rm M}=0.7$ are plotted as well.

4.2 Vertical chute flow

The uniform solid fraction and the uniform velocity in the core region are correctly reproduced by the model. Concerning the sheared regions closed to the vertical boundaries, the relative velocity profile (20) and the compaction profile (19) are quite similar to results gathered in Figures 7b and c of [14].

4.3 Heap flow

The solid fraction profile (10) and the velocity profile (12) are quite close to those represented in Figures 9b and c of [14] and in Figures 9a and b of [15]. In particular, the velocity profile displays a Bagnold-like profile very close to the free surface ($z < 0.2L(\theta)$), a quasi-linear profile in the central part of the flow ($0.2 < z/L(\theta) < 2$) and finally an exponential tail for the deepest parts of the flow, as observed in [16]. At variance with confined flows for which the shear was localized in boundary layers with thickness of the order of a few grain diameters, heap flows are characterized by a thickness $L(\theta)$ of a few grain diameters when θ is slightly larger than $\theta_{\rm min}$ but which increases to quite large values when θ is close to $\theta_{\rm max}$. A similar unlimited increase of the grain flux $Q_{\rm heap}$ is observed for θ close to $\theta_{\rm max}$, as seen in Figure 4. Such a behaviour is difficult to observe experimentally due to the limited values of $Q_{\rm heap}$ that can be achieved in usual laboratory devices. According to (6) and (11), our model predicts $L \sim (Q_{\rm heap})^{2/5}$

when θ is not too close to $\theta_{\min}$, a result slightly different from the scaling $L \sim (Q_{\rm heap})^{1/2}$ suggested by Figure 9j of [14].

4.4 Rough inclined planes

We explained the appearance of the so-called "immature sliding flows": they develop when the imposed flux $Q_{\rm plate}$ over a plate with inclination θ is larger than the flux $Q_{\rm heap}(\theta)$ which would fall down a heap with the same slope. Since $Q_{\rm plate}$ is experimentally limited to some maximum value, immature flows are observed for θ close to $\theta_{\min}$ only. When θ comes close to $\theta_{\max}$, the thickness h of the granular layer flowing over the rough incline becomes much smaller than the thickness of the grain layer which would flow down a heap with similar slope. And when h is less than $0.2L(\theta)$, the Bagnold-like velocity profile is invading the whole flowing layer, with the $h^{5/2}$ scaling for the flux $Q_{\rm plate}$ as a direct consequence (provided the first contribution to (14) is negligible). A different scaling, $h^{(5-\gamma)/2}$, is obtained with a different expression for $\mu_{\rm T}$ as discussed in Appendix B. The main drawback of our model is its inability to explain the quantity $h_{\rm stop}(\theta)$ introduced by Pouliquen [17] and which was confirmed in numerical simulations [18]. The first reason is that we assumed the friction coefficient μ to be independent of the solid fraction. As a consequence, $\theta_{\min}$ is a constant and $h_{\rm stop}$ vanishes as soon as $\theta > \theta_{\min}$. A second reason is the possible inadequacy of our model close to the rough incline. In this basal or frictional layer [6,13], the particle rotation plays an important role, the grain stress tensor is possibly non-symmetric and the solid fraction has a perturbed profile. All these phenomena would require a specific modelling. In fact the explanation of $h_{\rm stop}(\theta)$ proposed by Mills *et al.* [9] involves constitutive relations which are different close to the boundaries from those holding in the bulk. Concerning the solid fraction profile, the present model predicts a profile given by (10), gradually increasing from $\phi_{\rm m}$ at the free surface to $\phi_{\rm heap}(h/L(\theta))$ close to the rough plate. This prediction is in rather good agreement with the experimental profiles of Ancey [19] but is in contradiction with the simulations of Silbert *et al.* [18] who found a completely flat profile depending on θ but independent of z, hence of h.

4.5 Annular shear

This special kind of shear flow was not considered here because to describe it, we would need a constitutive equation for the τ_{xx} component of the granular stress, besides those for τ_{xz} and τ_{zz}. This will be done in future work.

5 Conclusion

We proposed a model for dense shear flows which considers the solid fraction as the main microstructural parameter. The granular stress is partitioned in a way similar to that proposed by Savage [12,4]. One of the distinctive features is a completely explicit expression for the contact stress which involves a function $F(\phi)$ of the solid fraction. The solid fraction profile mainly depends on the compressibility $\mathrm{d}F/\mathrm{d}\phi$ while the velocity gradient is bound to $F(\phi)/\mu_{\rm T}(\phi)$, where $\mu_{\rm T}(\phi)$ is somehow analoguous to the effective viscosity used by Bocquet *et al.* [7]. In principle the complete model contains two more functions of the solid fraction ($\mu(\phi)$ and $\mu_{\rm N}(\phi)$) but we strived to show that not so bad predictions could be obtained after assuming the friction coefficient μ and the dilatancy ratio $\mu_{\rm N}/\mu_{\rm T}$ to be independent of the solid fraction. Obviously, these are simplifying assumptions which can be released and improved. We also checked that the tentative (and simple) expressions (9) for $F(\phi)$ and $\mu_{\rm T}(\phi)$ led to sound predictions for the velocity and solid fraction profiles with one exception only, the compaction profile in flows down rough inclines.

The main drawback of constitutive equations (2) (or (15)) and (3) is their possible failure in a thin layer close to rough boundaries, *i.e.* at places where a couple stress and a relative angular velocity are likely to exist [20]. Their main advantage is to contain all the ingredients necessary to interpret the *bulk* shear-localization phenomenon, and to be able to explain in a qualitative way the quite different velocity profiles appearing in the stationary shear flows of dense granular materials.

Appendix A. Granular pressure

Close to the maximum compaction $\phi_{\rm M}$, the compressibility of the granular medium stems from a purely geometric effect, the number of different ways the grains can be distributed in space for a given volume fraction. This is reminiscent of the situation described by the cellular lattice-gas model. Starting from its free-energy per unit volume

$$\psi_{\rm lg} = \nu k_{\rm B} T[\tilde{\phi}\mathrm{Log}\tilde{\phi} + (1-\tilde{\phi})\mathrm{Log}(1-\tilde{\phi})]\,,$$

one deduces the lattice-gas configuration pressure

$$P_{\rm lg} = \frac{\partial \psi_{\rm lg}}{\partial \tilde{\phi}} = \nu k_{\rm B} T \mathrm{Log}\left(\frac{\tilde{\phi}}{1-\tilde{\phi}}\right)\,,$$

where ν is the number of cells per unit volume and $\tilde{\phi}$ is the fraction of cells occupied by particles. For granular materials, the thermal energy is replaced by the mechanical energy $F_0\rho_p g D$ and $\tilde{\phi}$ is replaced by $\phi/\phi_{\rm M}$. The main difference between the contact pressure and the lattice-gas pressure is that the contact pressure vanishes for ϕ smaller than $\phi_{\rm m}$, hence our expression (9) for $F(\phi)$. The analogy with the lattice-gas model is far from perfect and to improve the expression of $F(\phi)$ one can address to more sophisticated approaches such as the one developped by Blumenfeld and Edwards [21].

Appendix B. Influence of $\mu_{\mathrm{T}}(\phi)$ on scaling laws

The behaviour of $\mu_{\mathrm{T}}(\phi)$ close to the lowest compaction ϕ_{m} has a large influence on the predicted velocity profiles close to the free surface. Keeping the same expression (9) for $F(\phi)$, let us use a more general expression for μ_{T} in the form

$$\mu_{\mathrm{T}} = \mu_{\mathrm{T0}}(\phi_{\mathrm{M}} - \phi_{\mathrm{m}})^{2-\gamma}\frac{(\phi-\phi_{\mathrm{m}})^{\gamma}}{(\phi_{\mathrm{M}}-\phi)^2}$$

with a positive exponent γ because μ_{T} is not expected to diverge for $\phi = \phi_{\mathrm{m}}$. The compaction profiles of heap flows are unchanged but the velocity profiles close to the free surface now depend on exponent γ. Our numerical results for the velocity profiles can be fitted with a very good accuracy by an expression which generalizes (12)

$$1 - \frac{V_{\mathrm{heap}}(z)}{V_{\mathrm{heap}}(0)} = \left(\frac{\phi_{\mathrm{heap}}(z)-\phi_{\mathrm{m}}}{\phi_{\mathrm{M}}-\phi_{\mathrm{m}}}\right)^{\frac{3-\gamma}{2}} = \left(\frac{1-e^{-z/L(\theta)}}{1+(\frac{\phi_{\mathrm{M}}}{\phi_{\mathrm{m}}}-1)e^{-z/L(\theta)}}\right)^{\frac{3-\gamma}{2}}. \quad \text{(B.1)}$$

A region of inverse concavity exists close to the free surface when γ is less than one but it is only when γ is null that this region of inverse concavity has a Bagnold-like profile. When $\gamma = 1$ the velocity profile is quasi-linear up to the free surface [15,2] and when $1 < \gamma < 3$ there is no change of concavity but a large increase of the velocity close to the free surface [6]. A second consequence concerns flows over rough plates. When $h < 0.2L(\theta)$, result (14) is transformed into

$$\frac{Q_{\mathrm{plate}}}{D\sqrt{gD}} = \frac{\phi_{\mathrm{m}}V_{\mathrm{s}}h}{D\sqrt{gD}} + \frac{2}{5-\gamma}\phi_{\mathrm{m}}^{3/2}\left(\frac{(\sin(\theta)-\mu\cos(\theta))}{\mu_{\mathrm{T0}}}\right)^{1/2} \times \left(\frac{L(\theta)\phi_{\mathrm{M}}}{D\phi_{\mathrm{m}}}\right)^{\frac{\gamma}{5}}\left(\frac{h}{D}\right)^{\frac{5-\gamma}{2}}. \quad \text{(B.2)}$$

Measurements of $Q_{\mathrm{plate}}(h)$ by Ancey [19], Rajchenbach [2] and Pouliquen [17], respectively, suggest that $\gamma = 3, \gamma = 1$ and $\gamma = 0$. The issue is far from being settled.

References

1. E. Azanza, *Ecoulements granulaires bidimensionnels sur plan incliné*, Doctoral Thesis from Ecole Nationale des Ponts et Chaussées (1998).
2. J. Rajchenbach, Phys. Rev. Lett. **90**, 144302 (2003).
3. C. Ancey, P. Coussot, P. Evesque, Mech. Cohesive-frictional Mater. **1**, 385 (1996).
4. S.B. Savage, *Granular flows down rough inclines - review and extension*, in *Proceedings of US-Japan Seminar on New Models and Constitutive Relations in the Mechanics of Granular Materials*, edited by J.T. Jenkins, M. Satake (Elsevier Science Publishers, Amsterdam, 1982) pp. 261-282.
5. P.C. Johnson, R. Jackson, J. Fluid Mech. **176**, 67 (1987).
6. C. Ancey, P. Evesque, Phys. Rev. E **62**, 8349 (2000).
7. L. Bocquet, W. Losert, D. Schalk, T.C. Lubenski, J.P. Gollub, Phys. Rev. E **65**, 011307 (2002).
8. M.A. Goodman, S.C. Cowin, J. Fluid Mech. **45**, 321 (1971).
9. P. Mills, D. Loggia, M. Tixier, Europhys. Lett. **45**, 733 (1999); P. Mills, M. Tixier, D. Loggia, Eur. Phys. J. E **1**, 5 (2000).
10. I.S. Aranson, L.S. Tsimring, Phys. Rev. E **64**, 020301 (2001); D. Volfson, L.S. Tsimring, I.S. Aranson, Phys. Rev. Lett. **90**, 254301 (2003).
11. F. Da Cruz, F. Chevoir, J.-N. Roux, I. Iordanoff, *Macroscopic friction of dry granular materials*, in *Proceedings of the 30th Leeds-Lyon Symposium of Tribology*, edited by D. Dalmaz *et al.*, Tribology Series, Vol. **42** (Elsevier, 2003).
12. S.B. Savage, J. Fluid Mech. **377**, 1 (1998).
13. M.Y. Louge, Phys. Rev. E **67**, 061303 (2003).
14. G.D.R. Midi, *On dense granular flows*, to be published in Eur. Phys. J. E.
15. J. Rajchenbach, Adv. Phys. **49**, 229 (2000).
16. T.S. Komatsu, S. Inagaki, N. Nakagawa, S. Nasuno, Phys. Rev. Lett. **86**, 1757 (2001).
17. O. Pouliquen, Phys. Fluids **11**, 542 (1999).
18. L.E. Silbert, J.W. Landry, G.S. Grest, Phys. Fluids **15**, 1 (2003).
19. C. Ancey, Phys. Rev. E **65**, 011304 (2001).
20. K. Kanatani, Int. J. Eng. Sci. **17**, 419 (1979).
21. R. Blumenfeld, S.F. Edwards, *Granular entropy: Explicit calculations for planar assemblies*, cond-mat/0303418.